Mechanics of Advanced Composite Structures

Semnan University

journal homepage: http://MACS.journals.semnan.ac.ir

An Investigation of Stress and Deformation Behavior of Functionally Graded Timoshenko Beams subjected to Thermo-Mechanical Load

D. Mahapatra[a], S. Sanyal[b], S. Bhowmick[b,*]

[a] *Department of Mechanical Engineering, National Institute of Technology, Raipur, 491010, India*
[b] *BRSCAET&RS, Indira Gandhi KrishiVishwavidyalaya, Raipur, 495334, India*

KEYWORDS

Functionally graded beams
Timoshenko beams
Power law index
Thermo-mechanical load
Unified formulation

ABSTRACT

A functionally graded material beam with generalized boundary conditions is contemplated in the present study in order to examine the deformation and stress behavior under thermal and thermo-mechanical load. Three discrete combinations of functionally graded materials have been deliberate in including a wide range of materials and material properties. The variation of material properties has been taken along the height of the beam cross-section as per power law formulation. The formulation has been derived, applying the principle of virtual work in order to acquire governing equations for FG Timoshenko beams. The development of governing equations is made through applying a unique method of unified formulation (Li [16]) in which the displacement variables are arranged in the form of aindependent variable that subsequently reduces the equations to a single fourth order differential equation similar to the equation given by classical beam theoryand is been extended to thermo-mechanical loading in the present work. The transverse shear stress/ strain for Timoshenko beams have been taken care of within this unified formulation. The formulation employed in this research has been generalized for various loading conditions, and in the present work, thermal and thermo-mechanical load has been pondered where temperature has been varied in accordance with the beam height. Exact solutions of the fourth order differential equation for the deformation and stress have been obtained for three types of boundary conditions viz.- Clamped-Free (C-F), Simply Supported (S-S), and Propped Cantilever (C-S). The study has been extended to cover wide range of temperature distribution so as to include uniform, linear and non-linear temperature profiles. Deformation and stresses, axial stresses, and transverse (shear) stresses have been reported for different power law index values.

1. Introduction

The advent of Functionally Graded Materials as high grade composite materials has revolutionized the researches in Materials Technology in part and Engineering as a whole. The naturally existing FGMs like bamboo, human bones, tooth, etc. indicate superior characteristics in their behavior as a result of the gradual variation in their properties, which is the essence of FGMs. The concept of FGM has been employed in mid-1980s; however, the general idea of gradual variation of properties for composites germinated way back in early 1970s [1]. The most common FGM consists of a refractory ceramic and metal so as in order to acquire high temperature strength and toughness with minimal stress concentration and residual stresses. Contrary to the traditional composites that have sharp interfaces resulting in failures, the FGMs have continuous or gradual change in properties; hence there is no interface phenomenon observed in FGMs. FGMs are produced by tailoring the distribution of the ingredients or the structure in the desired fashion and in a particular direction. The most common method of producing FGMs is to change the composition of its material constituents (by volume). In such materials the composition (volume of constituents) is varied pursuant to a predefined manner so as to obtain a resultant of properties of the parent material, which is governed by the percentage by volume at that position. FGMs owing to their superior characteristics as above are contemplated as materials for broad future engineering applications from bio-medical, space technology, and many more.

* Corresponding author. Tel.: +91-9575 955040
E-mail address: sbhowmick.mech@nitrr.ac.in

DOI: 10.22075/MACS.2019.16748.1187
Received 2018-12-14; Received in revised form 2019-02-08; Accepted 2019-04-26

Beams and plates are an integral part of structures. When structures are exposed to severe environments, consequently to sustain such conditions the materials must exhibit superior properties. If we deliberate a space shuttle, while entering the earth's atmosphere, is exposed to very high temperature gradient through a small thickness. The extreme pressure and temperature gradient require stringent behavior prominently significant at the interface. The ceramic-metal based FGMs are especially suitable for such high temperature gradients with ceramic parts exposed to higher temperatures while the metal part ensures the FGM to gain its strength. The gradual change of material properties aids in sustaining the stress-concentration, and residual stresses developed otherwise. The design of such structural components requires a thorough analysis of load-deflection-stress behavior under various thermo-mechanical conditions and other related environmental factors.

Since their conceptualization, there had been substantially research on FGMs, and a large volume of publications on FGMs has been reported. A broad overview of the FGMs, their modeling and design, processing, and fabrication techniques and applications are employed in [1-5]. Birdman et al. [6] have investigated a number of critical areas relevant to the modeling and design of functionally graded materials in general and FG structures in particular. However, most of the studies pertinent to FG structures have been made in last two decades. The initiation of the studies pertinent to structural elements like beams and plates that are made up of FGMs may be credited to Reddy and Chin [7]. In their work they have contemplated a first order shear deformable plate made up of ceramic/metal FGM subjected to both mechanical and thermal load. Later the work was extended by Reddy [8] to incorporate third order shear deformation and von Karman type geometric non-linearity. Shankar [9] has reported the examination of FG Euler Beams with exponential grading of material constituents and hence, material properties. In [9] Shankar has applied the theory of elasticity approach to developing constitutive equations for FG beams subjected to sinusoidal loading and presented an exact solution. Various case studies correlated length/height ratio has been surveyed to distinguish the behavior of slender and stubby beams. Shankar et al. [10] have inquired the stresses as a result of the thermal gradient load applying theory of elasticity approach. In [11] Zhu and Shankar have presented approximate solutions using Fourier series and Galerkin method for deformation and stress analysis of FG beams subjected to sinusoidal mechanical load. There have been wide applications of finite element analysis to acquire approximate solution to examine the behavior of FG beams and plates, and substantially numbers of works have been inspected. A new beam finite element is developed by Chakraborty et al. [12] that can be applied in order to analyze the static and dynamic behavior of FG beams in thermal environment. A free vibration study of FG beams has been explored in [13], in which Aydogdu et al. have used Hamilton's principle to derive the governing equations and Navier type solutions for frequencies. Both exponential and power laws have been contemplated in this study for various slenderness ratios. Static behavior of FG beams applying higher order shear deformation theory has been examined by Kadoli et al. [14]; Benatta et al. [15] have employed higher order shear deformation theory to validate it for short FG beams. Li [16] has reported a unified formulation for shear deformable beams so as to study the static and dynamic behavior of FG beams; the study reports the behavior of Timoshenko beam and Rayleigh beam. Kang et al. [17] have inquired the behavior of FG beams taking into account material non-linearity and compared large and small deflection theories. Birman [18] has inspected the study of application of FG layer within two composite fiber layers with uni-axial load for buckling while Javaheri et al. [19] have applied biaxial loads to compute the critical buckling load of FG plates.

As ceramic-metal FG beams and plates are most suitable in high/severe temperature environments, this has leaded wide researches in the study of behavior of FG beams in thermal environment. It has been observed that most of these studies have considered temperature gradient (across the cross-section) load assuming the distribution of temperatures to be either linear or non-linear. The non-linear temperature distribution is acquired by solving one dimensional steady state heat transfer equation. These researches can be broadly classified into two types of studies viz. - coupled (or temperature dependent properties, TD) and uncoupled (temperature independent properties, TID). In the former case, material properties are functions of both space and temperature, while in the latter case they vary along the space only with an external temperature distribution overlapping on the system. Chin et al. [7], Praveen et al. [20], and Reddy [8] have surveyed the response of FG cylinders and plates in thermal load with thermo-mechanical coupled properties to report that uncoupled case over-estimates the temperature and stress fields. Shen [21] has investigated the non-linear bending response of FG plate subjected to mechanical load in thermal environment. Shen applied TD properties using higher order shear deformation theory and solution applying Galerkin's –perturbation theory. Shankar [10], in his study, has assumed exponential distribution of properties and of temperature (assuming TID case) and reported that there is reduction of thermal stresses if the gradation of temperature and that of material property are in the opposite direction. Sundararajan et al. [22] have studied vibration analysis of FGM plates using von Karman non-linearity and TD material properties; non-linear temperature distribution is assumed as well; material gradation using Mori-Tanaka scheme has been applied to compute the effective material properties. Li et al. [23] have inspected the thermal post-buckling analysis of FG beams considered the effect of shear deformation using geometrically non-linear formulation. The beam is subjected to both mechanical and TID thermal loading; temperature distribution being non-linear profile. Mahi et al. [24] have investigated exact solutions for free vibration analysis of symmetric FG beams with TD material properties. Three types of distributions viz. – power law, exponential and sigmoid variation are considered; in conformity with non-linear temperature distribution across the beam height. Nonlinear strain displacement relations are applied to derive the governing equations for buckling analysis under thermal load, and a number of publications are reported in this area. Javaheri et al. [25,26], Kiani et al. [27,28], Wattanasakulpong et al. [29], Majumdar et al. [30], Paul et al. [31] have examined the buckling of FG Beams using non-linear strain-displacement relations and non-linear temperature profiles.

The concept of physical neutral surface in FG beam analysis causes the stretching-bending coupling parameter vanishes in the governing equations, and the resulting equations are largely simplified. Applying this theory, the neutral surface is assumed to be one of the coordinate axes which hence is slightly shifted from the geometrical center. However, the geometrical middle surface and physical neutral surface coincide for isotropic/ homogenous beams. The concept of physical neutral surface has been utilized by Zhang et al. [32], Ma et al. [33, 34], and Fu et al. [35]. Different studies have been made on thermal analysis of beams that are resting on non-linear elastic foundations as- Fallah et al. [36] have examined the buckling analysis under thermo-mechanical load applying TID properties; Zhang et al. [37] have investigated the thermal post-buckling cases based on physical neutral surface and higher order shear deformation analysis using TD material properties; Sun et al. [38] have surveyed the study of thermal buckling of FGM Timoshenko beams with nonlinear temperature distribution and TID properties. Niknam et al. [39] have also inquired the thermo-mechanical loading effect on the behavior of non-linear FG tapered beams. Nasirzadeh et al. [40] have examined the stability conditions for FG beams in thermal and electrical field simultaneously and reported the results for various end conditions and power law indices. Nguyen et al. [41] have inspected the application of higher order hierarchal beam element for the dynamic analysis of FG beams subjected to non-linear temperature distribution along the cross-section height and TD material properties.

After an exhaustive review of the published works in the area of thermo-mechanical analysis of FG beams, it has been observed that studies pertinent to cumulative thermal and mechanical loading have been relatively less. Deliberating the scope of applications of beams in wide areas of severe/ critical standards the possibility of beams exposed to amalgamated thermal and mechanical loading cannot be foreseen. In other words, when an FG beam is subjected to constant mechanical load in thermal environment the study of deformation and stresses with changes in temperature distribution can be quite significant in its design analysis and synthesis. The present work reveals the effect of change of temperature distribution on stress and deformation behavior of an FG Timoshenko beam loaded with a constant mechanical load. The governing equations are derived applied principle of virtual work in the frame of Timoshenko beam theory to incorporate transverse shear strains in thermal environment. The formulation is derived applying the unified approach as reported by Li [16] in which a single governing equation is derived by reducing the three differential equations of displacement variables into a single fourth order equation. Poisson's ratio is assumed to be a constant and material properties are assumed to be independent of temperature change. Exact solutions are acquired, assuming beam to be subjected to various boundary conditions. Three types of FG materials viz.- Aluminum/Steel (metal-metal), Stainless Steel/ Silicon Nitride(metal-ceramic) and Stainless Steel/ Zirconia (metal-ceramic) have been contemplated in the study under linear and non-linear distribution of temperatures and for dissimilar ranges of temperatures and volume concentrations of material constituents.

2. Formulation

2.1. Modeling of Functionally Graded Materials

A functionally graded beam of length 'L,' rectangular dimensions of width 'b,' and height 'h,' having three dimensional Cartesian coordinate systems as illustrated in Fig. 1 and material property gradation across the cross-section is reviewed for static analysis. This beam is assumed to be loaded uniformly with a constant load intensity 'q' kN/m.

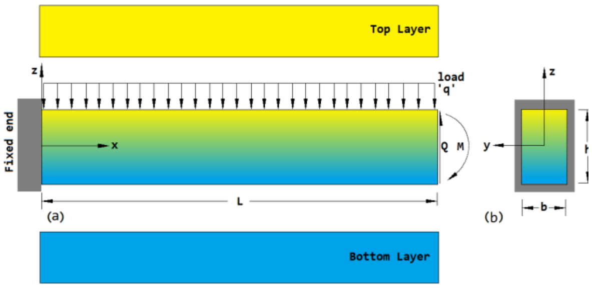

Fig. 1. Schematic diagram of FG beam and its coordinate system (a) Front view (b) Side view

A thermal field is also assumed in such a way that the temperature of top surface and bottom surface is prescribed initially; the variation of temperature is assumed to be uniform, linear, or non-linear, depending on the case assumed. Functionally Graded Materials are advanced composite materials whose properties are tailored in a desired manner to obtain specific properties. The composition of the parent materials is varied in a specified manner to achieve such variation in the properties. In this paper the variation of material properties is assumed to be in consonance with power law function and simultaneously the beam height. The expression for power law is presented by (e.g. see Fig. 2):

$$P(z) = P_b + (P_t - P_b).\left(\frac{z}{h} + \frac{1}{2}\right)^{\beta} \quad (1)$$

where '*P*' is any material property, '*z/h*' represents the normalized distance from geometrical center.

The subscripts '*b*' and '*t*' refers bottom and top fiber, respectively, and '*β*' is the power law index. As the Table 1 displays, the values of Poisson's ratio for the materials are very close to each other. In order to keep the analysis simpler, Poisson's ratio is assumed to be constant. However, to generalize the idea to wider arena, the variation of Poisson's ratio (*(z)*, where its variation is as per power law depth dependent) can be easily be incorporated in the governing equations. The effect of variation of Poisson's ratio will be observed in rigidity modulus and shear correction factors [16] as presented below-

$$G(z) = \frac{E(z)}{2(1+\mu(z))} \quad (2)$$

$$k_s(z) = \frac{5(1+\mu(z))}{(6+5\mu(z))} \quad (3)$$

2.2. Governing Equations

The above beam is deliberate to be Timoshenko beam i.e., the effect of shear deformation will be accounted for the displacement variables; loading and corresponding deflection is constrained in the x-z plane. Let '*u*,' '*w*,' and ϕ represent the axial and transverse deflection and rotation of the cross-section at the mid-plane, respectively. A subscript '0' with the variable (for e.g. u_0) will account for the corresponding variable value at mid-plane. The transverse deflection '*w*' and the shear deformation '*γ*' are assumed to be functions of '*x*' and are uniform for a cross-section.

Based on Timoshenko beam theory-

$$u(x,z) = u_0(x) + z\phi(x) \quad (4)$$

$$\epsilon_{xx} = \frac{\partial u}{\partial x} = \frac{\partial u_0}{\partial x} + z\frac{\partial \phi}{\partial x} - \alpha(z)[T(z)\text{-}T_0] \quad (5)$$

$$\gamma_{xz} = \phi + \frac{\partial w}{\partial x} \quad (6)$$

In the above equations ϵ_{xx} and γ_{xz} represent the normal and shear strain respectively, *α(z)* is the coefficient of thermal expansion, and *T(z)* is the temperature; both of these depend on the material configuration shown by power law equation (Eq. 1). T_0 is reference temperature. Virtual work principle states that the variation in strain energy is equal to the work done by the load to cause an infinitesimal deflection of beam, i.e.:

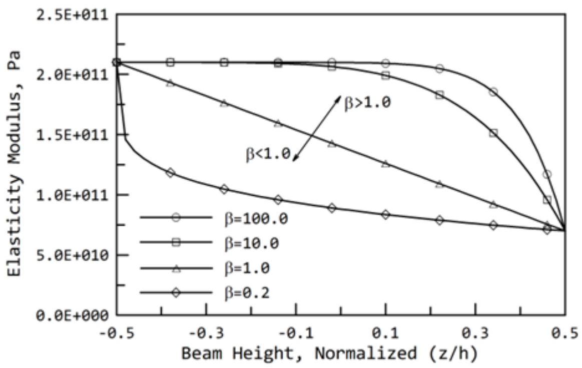

Fig. 2. Variation of Modulus of Elasticity across the cross-section with power law index, *β*

Table 1. Mechanical Properties of Materials

Material	μ	E (GPa)	α x10^{-6} (^{0}C^{-1})	K (Wm^{1}K^{-1})	Ref.
Steel	0.3000	207	12.3	51.90	[42]
Aluminum	0.3300	69	23.6	222.00	[42]
Stainless Steel	0.3262	201.04	12.330	15.379	[7]
Silicon Nitride	0.2400	348.43	5.8723	13.7230	[7]
Zirconia	0.2882	244.27	12.766	1.7000	[7]

$$\delta U=\iint_0^L(\sigma_{xx}.\delta\epsilon_{xx}+\tau_{xz}.\delta\gamma_{xz}).dx.dA....$$
$$....+\int_0^L q.\delta w.dx=0 \quad (7)$$

$$\sigma_{xx}=E(z).\epsilon_{xx} \quad (8)$$

$$\tau_{xz}=k_s.G(z).\gamma_{xz} \quad (9)$$

$$dA=b.dz \quad (10)$$

$$\delta U=\iint_0^L\{(E(z).\epsilon_{xx}.\delta\epsilon_{xx}....$$
$$....+G(z).\gamma_{xz}.\delta\gamma_{xz})\}.dx.b.dz....$$
$$....-\int_0^L q.\delta w.dx=0 \quad (11)$$

The thermal force and thermal moment can be expressed as-

$$N_x=\int_{-h/2}^{h/2}\sigma_{xx}b.dz$$
$$N_x=\int_{-h/2}^{h/2}b.\left\{E(z)\left(\frac{du_0}{dx}+z\frac{d\phi}{dx}-\alpha(z)\Delta T(z)\right)\right\}.dz \quad (12)$$

$$M_x=\int_{-h/2}^{h/2}z\sigma_{xx}b.dz$$
$$M_x=\int_{-h/2}^{h/2}b.\left\{E(z)\left(z\frac{du_0}{dx}+z^2\frac{d\phi}{dx}-z\alpha(z)\Delta T(z)\right)\right\}.dz \quad (13)$$

Eqs. (14-17) are introduced for the decoupling of '*x*' and '*z*' parameters.

$$A_{11}=\int_{h/2}^{-h/2}E(z).1.dz \quad (14)$$

$$B_{11}=\int_{h/2}^{-h/2}E(z).z.dz \quad (15)$$

$$D_{11}=\int_{h/2}^{-h/2}E(z).z^2.dz \quad (16)$$

$$K_{55}=\int_{-h/2}^{h/2}k_s.G(z).dz \quad (17)$$

Here 'k_s' is the shear correction factor. Substituting the decoupling parameters in Eqs. 12 and 13 to acquire-

$$N_x=A_{11}\frac{du_0}{dx}+B_{11}\frac{d\phi}{dx}-N_T \quad (18)$$

$$M_x=B_{11}\frac{du_0}{dx}+D_{11}\frac{d\phi}{dx}-M_T \quad (19)$$

$$Q_{xz}=\int_{-h/2}^{h/2}\sigma_{xz}dA=K_{55}\left(\phi+\frac{dw}{dx}\right) \quad (20)$$

After substituting for N_x and M_x in Eq. 11, followed by simplification and grouping of similar quantities, the following governing equations (Eqs. 21-23) are obtained-

$$\frac{\delta U}{\delta u}=\frac{dN_x}{dx}=A_{11}\frac{d^2u_0}{dx^2}+B_{11}\frac{d^2\phi}{dx^2}-\frac{dN_T}{dx}=0 \quad (21)$$

$$\frac{\delta U}{\delta\phi}=\frac{dM_x}{dx}-Q_{xz}=0$$
$$=B_{11}\frac{d^2u_0}{dx^2}+D_{11}\frac{d^2\phi}{dx^2}+$$
$$K_{55}\left(\phi+\frac{dw}{dx}\right)-\frac{dM_T}{dx}=0 \quad (22)$$

$$\frac{\delta U}{\delta w}=\frac{dQ_{xz}}{dx}+q=K_{55}\left(\frac{d\phi}{dx}+\frac{d^2w}{dx^2}\right)+q=0 \quad (23)$$

The following boundary conditions are computed (Eq. 24-26)-

$$(N_x=0)or(\delta u=0) \quad (24)$$

$$(M_x=0)or(\delta\phi=0) \quad (25)$$

$$(Q_{xz}=0)or(\delta w=0) \quad (26)$$

In the above Eqs. (21-23), N_T represents the thermal force; M_T is the thermal moment shown by-

$$N_T=\int_{-h/2}^{h/2}E(z).\alpha(z).\Delta T(z).dA \quad (27)$$

$$M_T=\int_{-h/2}^{h/2}z.E(z).\alpha(z).\Delta T(z).dA \quad (28)$$

Equations (21-23) are governing differential equations and Eqs. (24-26) are respective boundary conditions for functionally graded beams whose solutions provide an insight to their static responses under dissimilar conditions of thermo-mechanical load. It can be observed from Eqs. 27 and 28 that thermal force and moment vary only accompanying the beam height and are independent of '*x*'; hence, the last term of Eqs. 21 and 22 vanish. On that account, the governing equations for thermo-mechanical load remain exactly similar to the case of purely mechanical load. The governing equations contain three variables viz. – u, w, and ϕ and can be simplified to reduce it into two variable formulations; i.e. if Eq. 21 is substituted in Eq. 22, it eliminates 'u_0', and the remaining equations are coupled with two parameters, viz. 'w' and.'' The following substitutions applying an independent variable 'F' (Reference [16]) can be incorporated to reduce it to a single variable equation.

$$w=F-\frac{D^*}{K_{55}}\frac{d^2F}{dx^2} \quad (29)$$

$$\phi = \frac{dF}{dx} \tag{30}$$

In the above equations *'F'* is an auxiliary function similar to transverse deflection and is applied only for simplification; while D* is a material property and a function of '*z*' only and is given by-

$$D^* = D_{11} - \frac{B_{11}^2}{A_{11}} \tag{31}$$

After the above substitutions, the governing equation for a shear deformable FG Timoshenko beam under thermo-mechanical load is reduced to a single fourth order differential equation as follows-

$$D^* . \frac{\partial^4 F}{\partial x^4} + q = 0 \tag{32}$$

Using Eqs. 22 and 23 the bending moment and shear force will take the form-

$$M_x = D^* \frac{\partial^2 F}{\partial x^2} + \frac{B_{11}}{A_{11}} N_T - M_T \tag{33}$$

$$Q_{xz} = D^* \frac{\partial^3 F}{\partial x^3} \tag{34}$$

Equation33 is acquired after assuming that the net axial force vanishes, which is the case for cantilever beams, propped beams, and simply supported beams (with at least one roller support in the latter). Once the independent variable '*F*' is computed, the other dependent variables can easily be determined. Exact solution of Eq. 32 is derived for each of the above three boundary conditions after contemplating the beam to be loaded with constant mechanical load in thermal environment.

2.3. Temperature Profile

The top surface is assumed to be at temperature, Tt, while the bottom surface temperature is T_b. Here it is assumed that $T_t<T_b$. Both T_t and T_b are more significant than the ambient temperature T_0. Three temperature profiles are deliberated in the present study- uniform temperature rise, linear temperature distribution, and non-linear temperature distribution. Generally, the temperature distribution in a component is computed applying steady state heat conduction equation, assuming the heat flow to be one-dimensional along the beam height. In a limiting case when beam is slender the temperature distribution can be approximated to be linear in accordance with the beam height.

2.3.1. Linear temperature distribution(LTD)

The two surfaces (top and bottom) of the beam are assumed to be at an initial temperature that is higher than the surroundings, and the temperature distribution is assumed to follow a linear distribution pursuan to the expression-

$$T(z) = T_b + (T_t - T_b).\left(\frac{z}{h} + \frac{1}{2}\right) \tag{35}$$

If both the temperature T_t and T_b are kept at same value (i.e., the entire beam temperature is same) and higher than the ambient temperature, will also lead to bending as a result of uneven thermal expansion as the constituents have different expansion coefficients which are a limiting case of uniform temperature rise.

2.3.2. Non-linear temperature distribution (NLTD)

Assuming there is no heat generation and heat flows uni-directionally from the bottom layer to the top layer such that it follows steady state one dimensional heat conduction equation shown by -

$$\frac{d}{dz}\left(K(z)\frac{dT}{dx}\right) = 0, T_{(-h/2)} = T_b, T_{(h/2)} = T_t \tag{36}$$

In the above equation, *K(z)* is the thermal conductivity of FGM at any point along the cross-section. The variation of thermal conductivity is assumed to be given by Eq. 1, as well. Eq. 36 can be solved applied polynomial series solution [25, 26, 28] and assuming that the first seven terms (N_p) of the series provide accurate solutions, the temperature profile across the beam height is:

$$T = T_b + \frac{(T_t - T_b)}{R}\left[\sum_{i=0}^{N_p} \frac{(-1)^i}{i\beta + 1}\left(\frac{K_{tb}}{K_b}\right)^i \left(\frac{1}{2} + \frac{z}{h}\right)^{i\beta+1}\right] \tag{37}$$

where-

$$R = \sum_{i=0}^{N_p} \frac{(-1)^i}{i\beta + 1}\left(\frac{K_{tb}}{K_b}\right)^i \quad \text{and } K_{tb} = K_t - K_b \tag{38}$$

3. Solution of Governing Equation

Equation 32 represents the governing equation of a shear deformable FG Timoshenko beam subjected to mechanical load in thermal environment. It is also observed that for those beam end conditions in which the axial force is negligible, the bending moment is a function of thermal load and moment as given by Equation 33. This is the same for three end conditions viz. – a) cantilever or clamped-free (C-F); b) propped cantilever or clamped-simply supported (C-S) and c) Simply supported-simply supported (S-S). In order to have zero axial force one of the ends must be free to move in horizontal direction; hence the present study focuses on these end conditions only.

3.1. Solution procedure

Integration of the governing equation of FG beams (Eq. 32) leads to the following solution-

$$\frac{\partial^3 F}{\partial x^3} = \frac{q}{D^*}x + C_1 \tag{39}$$

$$\frac{\partial^2 F}{\partial x^2} = \frac{q}{D^*}\frac{x^2}{2} + C_1 x + C_2 \tag{40}$$

$$F = \frac{q}{D^*}\frac{x^4}{24} + C_1\frac{x^3}{6} + C_2\frac{x^2}{2} + C_3 x + C_4 \tag{41}$$

where C_j *(j=1,2,3,4)* are constants to be computed from the end conditions. In the present study, three boundary conditions are deliberated as above to find the exact solution for thermo-mechanical loading of FG Timoshenko beams. The beams are subjected to an external uniform mechanical pressure of *'q'* kN/m intensity throughout the span and are also subjected to various temperature distributions superimposed on the beam. The constants may be computed applying the specified boundary conditions and *'F'* can be acquired easily. Once *'F'* is determined transverse deflection and rotation of cross-section can be obtained using Eqs. 29 and 30. The resulting deformations and stresses are observed hereafter for a wide range of parameters.

3.2. Various end conditions

3.2.1. Clamped-Free (C-F)

For a cantilever beam slope and deflection at the fixed end are zero while shear force and bending moment at the free end are zero. Hence we have the following end conditions for a C-F beam-

$$w(0) = \phi(0) = 0, M_x(l) = Q_{xz}(l) = 0 \tag{42}$$

The above boundary condition (Eq. 41) can be substituted by Eqs. 29, 30, 33 and 34 respectively in order to acquire the following-

$$\left(F - \frac{D^*}{K_{55}}\frac{d^2F}{dx^2}\right)_{x=0} = \left(\frac{dF}{dx}\right)_{x=0} = \left(D^*\frac{\partial^2 F}{\partial x^2} + \frac{B_{11}}{A_{11}}N_T - M_T\right)_{x=l} = \left(D^*\frac{\partial^3 F}{\partial x^3}\right)_{x=l} = 0 \tag{43}$$

Substituting the Eqs. 39-41 in Eq. 43 to obtain four simultaneous linear equations in C_j *(j=1,2,3,4)* which can be solved easily to obtain-

$$w = \frac{q}{24D^*}\left(x^4 - 4lx^3 + 6l^2x^2\right) - \frac{q}{2K_{55}}\left(x^2 - 2lx\right) + \frac{x^2}{2D^*}\left(\frac{B_{11}}{A_{11}}N_T - M_T\right) \tag{44}$$

and using Eqs. 5 & 8-

$$\sigma_{xx} = \frac{E(z)}{2D^*}\left(\frac{B_{11}}{A_{11}} - z\right)\left\{\begin{matrix} q\left(x^2 - 2lx + l^2\right) \\ -\left(\frac{B_{11}}{A_{11}}N_T - M_T\right)\end{matrix}\right\} + \frac{E(z)N_T}{A_{11}} - E(z)\alpha(z)\Delta T(z) \tag{45}$$

Applying the axial stresses obtained in Eq. 45, shear stresses can easily be derived by integrating-

$$\sigma_{xz} = \int_{-h/2}^{z} \frac{d\sigma_{xx}}{dx}dz \tag{46}$$

Hence an expression for shear stress is obtained as-

$$\sigma_{xz} = \frac{q}{D^*}(l - x)\left[\int_{-h/2}^{z} zE(z)dz - \frac{B_{11}}{A_{11}}\int_{-h/2}^{z} E(z)dz\right] \tag{47}$$

The above Eqs. 44-45 and 47 represent respectively the transverse deflection, normal stresses and shear stresses in an FG Timoshenko Beam subjected to thermo-mechanical load with C-F boundary conditions. It is clear from Eqs. 44 and 45 that in the absence of mechanical load (*q=0*), the transverse deflection and axial stresses are non-zero. On the other hand, if thermal load is zero (i.e. surface temperatures are equal to ambient temperature) then the Eqs. (44-47) exactly resemble that of Reference [16]. For isotropic beams $D^*=EI$, $K_{55} = k_sGA$, and $B_{11}=0$, hence for isotropic materials the above equations are reduced to-

$$w = \frac{q}{24EI}\left(x^4 - 4lx^3 + 6l^2x^2\right) - \frac{q}{2k_sGA}\left(x^2 - 2lx\right) - \frac{x^2 M_T}{2EI} \tag{48}$$

$$\sigma_{xx} = \frac{qz}{2I}\left(x^2 - 2lx + l^2\right) + \frac{M_T z}{I} + \frac{N_T}{A} - E\alpha(T - T_0) \tag{49}$$

For isotropic beams, the last two terms of Eq. 49 are equal and hence cancel each other, and terms with thermal moment are acquired. The above equations can be easily verified from standard text-books [42, 43].

3.2.2. Clamped-Simply supported (C-S)

For a propped cantilever beam (C-S) slope and deflection at the fixed end are zero while transverse deflection and bending moment at the roller ends are zero. Hence we have the following end conditions for a C-S beam-

$$w(0)=\phi(0)=0, w(l)=M_x(l)=0 \quad (50)$$

The above boundary condition (Eq. 50) can be substituted by Eqs. 29, 30, 33 and 34 respectively to obtain the following-

$$\left(F-\frac{D^*}{K_{55}}\frac{d^2F}{dx^2}\right)_{x=0}=\left(\frac{dF}{dx}\right)_{x=0}=$$
$$\left(F-\frac{D^*}{K_{55}}\frac{d^2F}{dx^2}\right)_{x=l} \quad (51)$$
$$=\left(D^*\frac{\partial^2F}{\partial x^2}+\frac{B_{11}}{A_{11}}N_T-M_T\right)_{x=l}=0$$

Solving the simultaneous equations obtained by substitution of Eqs. 39-41 in 51 which can be simplified to obtain the expressions for deflection and stresses as below-

$$\xi.w=\frac{q}{144D^*}\left(2x^4l^2-5x^3l^3+3x^2l^4\right)+....$$
$$....\frac{q}{24K_{55}}\left(x^4-4x^2l^2-2x^3l+5l^3x\right)....$$
$$....-\frac{qD^*}{2K_{55}^2}\left(x^2-lx\right)-\frac{T_l}{12D^*}\left(x^3l-x^2l^2\right).... \quad (52)$$
$$-\frac{T_l}{2K_{55}}\left(x^2-lx\right)$$

$$\sigma_{xx}=\frac{E(z)}{\xi}\left(\frac{B_{11}}{A_{11}}-z\right)\left\{\begin{array}{l}\frac{q}{24D^*}\left(4x^2l^2-5xl^3+l^4\right)\\ -\frac{q}{2K_{55}}\left(x^2-lx\right)-\\ \frac{T_l}{2D^*}\left(xl-\frac{l^2}{3}\right)-\frac{T_l}{K_{55}}\end{array}\right\} \quad (53)$$
$$+\frac{E(z)N_T}{A_{11}}-E(z)\alpha(z)\Delta T(z)$$

$$\xi.\sigma_{xz}=\left[\begin{array}{l}\frac{q}{24D^*}\left(8xl^2-5l^3\right)\\ +\frac{q}{2K_{55}}\left(2x-l\right)\\ -\frac{T_l l}{2D^*}\end{array}\right] \quad (54)$$
$$\left\{\int_{-h/2}^{z}zE(z)dz-\frac{B_{11}}{A_{11}}\int_{-h/2}^{z}E(z)dz\right\}$$

The following substitutions have been made in Eqs. 52-54

$$\xi=\frac{l^2}{3}+\frac{D^*}{K_{55}}$$
$$T_l=\left(\frac{B_{11}}{A_{11}}N_T-M_T\right) \quad (55)$$

If we neglect the effect of shear deformation in the above analysis for C-S beam, hence the corresponding beam will be Euler-Bernoulli beam (EBB). For such beams the value of K_{55} will be infinite hence the value of $\xi=l^2/3$ and its substitution in Eqs. 52-54 will simplify them to those for EB beams-

$$w=\frac{q}{48D^*}\left(2x^4-5x^3l+3x^2l^2\right)-\frac{T_l}{4D^*}\left(\frac{x^3}{l}-x^2\right) \quad (56)$$

$$\sigma_{xx}=E(z)\left(\frac{B_{11}}{A_{11}}-z\right)\left\{\begin{array}{l}\frac{q}{8D^*}\left(4x^2-5xl+l^2\right)....\\ ....-\frac{T_l}{2D^*}\left(\frac{3x}{l}-1\right)\end{array}\right\} \quad (57)$$
$$+\frac{E(z)N_T}{A_{11}}-E(z)\alpha(z)\Delta T(z)$$

$$\sigma_{xz}=\left[\begin{array}{l}\frac{q}{8D^*}(8x-5l)....\\ ....+-\frac{3T_l}{2D^*l}\end{array}\right] \quad (58)$$
$$\left\{\int_{-h/2}^{z}zE(z)dz-\frac{B_{11}}{A_{11}}\int_{-h/2}^{z}E(z)dz\right\}$$

Further, if the beam is assumed to be isotropic then the following substitutions can be made- $D^*=EI$, $K_{55}=k_sGA$, and $B_{11}=0$, as in the previous case. It has been observed that the resulting equations for isotropic beam with C-F boundary condition, consequently the resulting /equations for transverse deflection, axial and shear stress are exactly similar to that in [43].

3.2.3. Simply supported -Simply supported (S-S)

A similar analysis as above for S-S type boundary condition whose at least one end is roller supported is discussed in this section. The boundary conditions associated with such beam are as below-

$$w(0)=M_x(0)=0, w(l)=M_x(l)=0 \quad (59)$$

Equation 59 can be converted into a relevant form by substitution of Eqs. 29 & 33 as-

$$\left(F-\frac{D^*}{K_{55}}\frac{d^2F}{dx^2}\right)_{x=0}=\left(\begin{array}{l}D^*\frac{\partial^2 F}{\partial x^2}+\\ \frac{B_{11}}{A_{11}}N_T-M_T\end{array}\right)_{x=0}=0$$
$$\left(F-\frac{D^*}{K_{55}}\frac{d^2F}{dx^2}\right)_{x=l}=\left(\begin{array}{l}D^*\frac{\partial^2 F}{\partial x^2}+\\ \frac{B_{11}}{A_{11}}N_T-M_T\end{array}\right)_{x=l}=0 \quad (60)$$

The final expressions obtained for transverse deflection and stresses after solution and simplification of the linear simultaneous equations (using Eqs. 39-41) acquired as follows-

$$w=\frac{q}{24D^*}\left(x^4-2x^3l+xl^3\right)-....$$
$$....\frac{q}{2K_{55}}\left(x^2-xl\right)-\frac{T_l}{2D^*}\left(x^2-lx\right) \quad (61)$$

$$\sigma_{xx}=\frac{E(z)}{2D^*}\left(\frac{B_{11}}{A_{11}}-z\right)\left\{q\left(x^2-lx\right)+2T_l\right\}....$$
$$....+\frac{E(z)N_T}{A_{11}}-E(z)\alpha(z)\Delta T(z) \quad (62)$$

$$\sigma_{xz}=\frac{q}{2D^*}(l-2x)$$
$$\left[\int_{-h/2}^{z}zE(z)dz-\frac{B_{11}}{A_{11}}\int_{-h/2}^{z}E(z)dz\right] \quad (63)$$

4. Results and Discussions

In order to gain a deep insight into the behavior of FG beams when it is subjected to mechanical load, and the temperature distribution across the beam height is varied, a number of numerical results based on the above analysis are presented in this section. In order to provide a clear perspective, the examination has been categorized into different cases so that the behavior of FG beam is investigating by varying one of the parameters (relevant to FGM) with a progressive rise of temperature and TID properties. The parameters that are of interest are- a) volume fraction of constituents governed by power law index, β (Eq. 1); b) comparison of different material combinations for constituents and hence material properties (Eq. 1); c) comparison of EB and Timoshenko beams for the same aspect ratio (l/h); d) linear and non-linear temperature profiles (Eqs. 35 & 38). A comparison of variation in load parameters viz. - purely mechanical/ purely thermal/ thermo-mechanical behavior has been employed for four sets of temperature ranges. Three combinations of FGM has been selected for study viz. – a) Metal-metal FGM applying Aluminum-Steel; b) Metal- Ceramic$_1$ using Stainless Steel and Silicon Nitride; c) Metal-ceramic$_2$ applying Stainless Steel and Zirconia; their nomenclature as FGM-1, FGM-2, and FGM-3 respectively. The study of behavior of FG beams with different end conditions (Section 3) has also been concluded. For computational purpose a beam of length L = 0.5 m and height h = 0.125 m, temperature of the surroundings T_0 = 30 ^oC, and uniform pressure of intensity q = 10 kN/m have been assumed. The material properties are mentioned in Table 1. The temperature of the top and bottom surfaces are kept at constant values and observations are made for four sets of temperature as mentioned in Table 2. The axial stresses and shear stresses are normalized using the following relations-

$$\sigma_{norm}=\frac{(\sigma_{xx}bh)}{ql+N_T};\tau_{norm}=\frac{(\sigma_{xz}bh)}{ql+N_T} \quad (64)$$

It is observed that even with the slightest of the rise in temperature of surface (above ambient temperature), results in appreciable variations in the deformation and stress features of FG beam. For instance, when the above FG beam (cantilever end condition) is kept near a heat source such that the temperature of bottom surface rises by 1^{0}C and let us assume that the temperature of top surface is same as the ambient, then the thermal gradient (assumed to be linear in this case) induces a net moment (due to the difference in coefficient of thermal expansion of the layers) that deflects the beam in upward direction. Notwithstanding, as the temperature of the top surface rises by 1^{0}C the deflection is again in downward sense as well. Thus, a small rise in temperature will cause significant changes in the behavior of the FG beam. Fig. 3(a-b) are plotted in order to detect the deflection and stresses corresponding to a unit rise of temperature. FGM-1 is metal –metal composite with Aluminum at the top and Steel at the bottom. When the bottom layer is heated above ambient (T_{bot}=31^{0}C, T_0=30^{0}C, T_{top} = 30^{0}C), it expands while the top layer being at ambient temperature remains un-deformed. This results in deflection of beam in upward direction.

Table 2. Symbols for temperature distribution

Temperature	Symbol	
	Uniform	
T_t=31^{0}C, T_b=31^{0}C	TU$_1$	
T_t=33^{0}C, T_b=33^{0}C	TU$_2$	
T_t=35^{0}C, T_b=35^{0}C	TU$_3$	
T_t=37^{0}C, T_b=37^{0}C	TU$_4$	
	Linear	Nonlinear
T_t=31^{0}C, T_b=31^{0}C	TL$_1$	TNL$_1$
T_t=31^{0}C, T_b=33^{0}C	TL$_2$	TNL$_2$
T_t=31^{0}C, T_b=35^{0}C	TL$_3$	TNL$_3$
T_t=31^{0}C, T_b=37^{0}C	TL$_4$	TNL$_4$

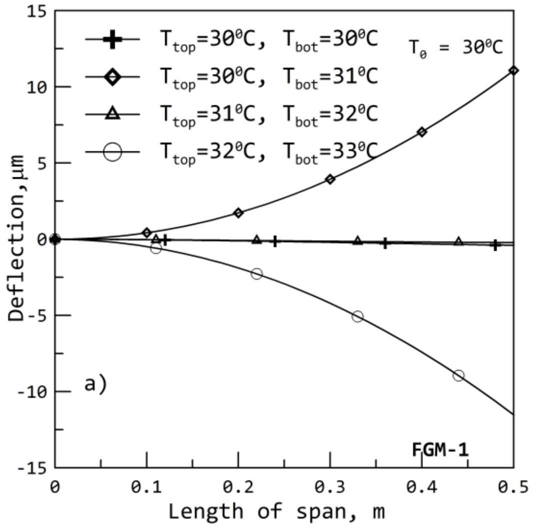

(a)

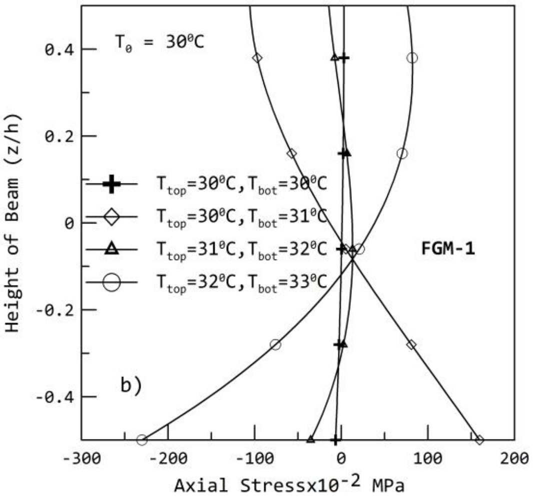

(b)

Fig. 3. a) Transverse Deflection b) Normalized Axial Stress (at the fixed end) of C-F beam (FGM-1) for $\boldsymbol{\beta}$=1

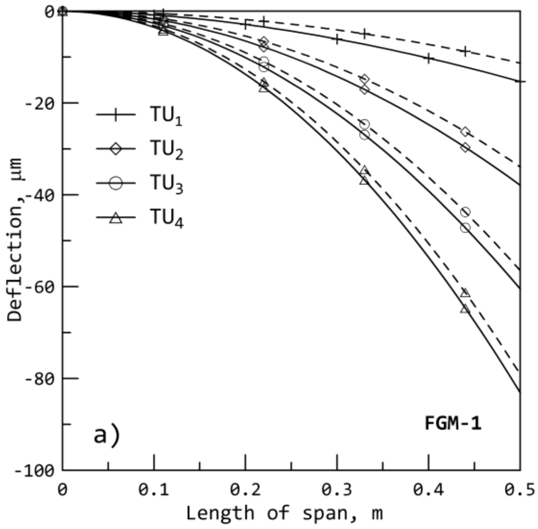

(a)

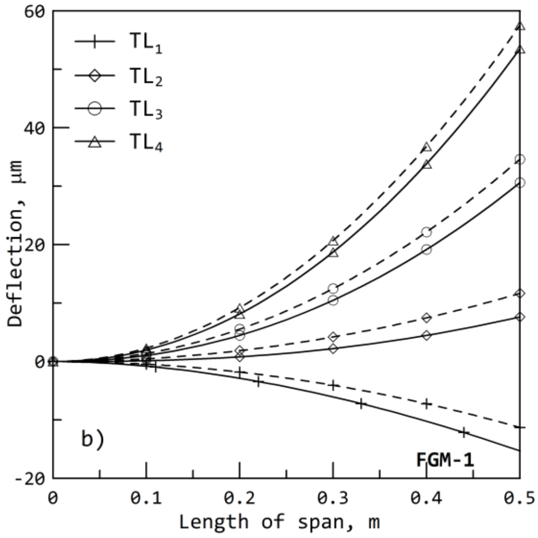

(b)

Fig. 4. Transverse Deflection of C-F beam (FGM-1) for $\boldsymbol{\beta}$=1
a) Uniform temperature; b) Linear Temperature Distribution

In the other case, (T_{bot}=33⁰C, T_0=30⁰C, T_{top} = 32⁰C) both the top and bottom layer expand due to heating; however, expansion of top layer is more than the bottom owing to the fact that thermal conductivity of aluminum is more (almost double) than that of steel. Hence the beam bends in the downward direction. In order to gain a broader view of such changes in their behavior, the values of temperatures for uniform, linear, and non-linear distribution are judiciously selected.

The following figures highlighted the behavior of FG cantilever beam subjected to thermo-mechanical loading. Figures 4-12 are plotted for FGM-1 and the subsequent figures (Figs. 13-16) represent comparative behaviors of FGM-1, 2, and 3. In order to distinguish the thermal and thermo-mechanical behavior, the thermo-mechanical graphs (q=10 kN/m) are plotted with solid lines while thermal plots (q=0 kN/m) are with dashed lines.

In Figs. 4-7, the value of power law index is kept constant (β=1), and temperature of top and bottom surfaces are varied.

Figs. 4a and 4b illustrate the deflection curves for uniform and linear distribution of temperature while Fig. 7b for nonlinear distribution. It is clearly observed that there is substantial difference in deflections in the above cases. In 4a, even with a uniform rise of temperature (T_t=T_b>T_0) above ambient, the beam bends; this may be attributed to the dissimilarity in the expansion coefficients of the constituents. If the loading side is reversed then results are in opposite sense as expected, but their magnitudes are different. Furthermore, the thermal deflection in each case is slightly less than thermo-mechanical because the thermal moment is opposite to mechanical moment (for FGM-1, aluminum is in top layer, and its thermal expansion is much higher as compared to steel).

It can be observed from Fig. 4b that for linear variation of temperature, the bending can be in the upward direction for thermo-mechanical case even for small temperature gradients.

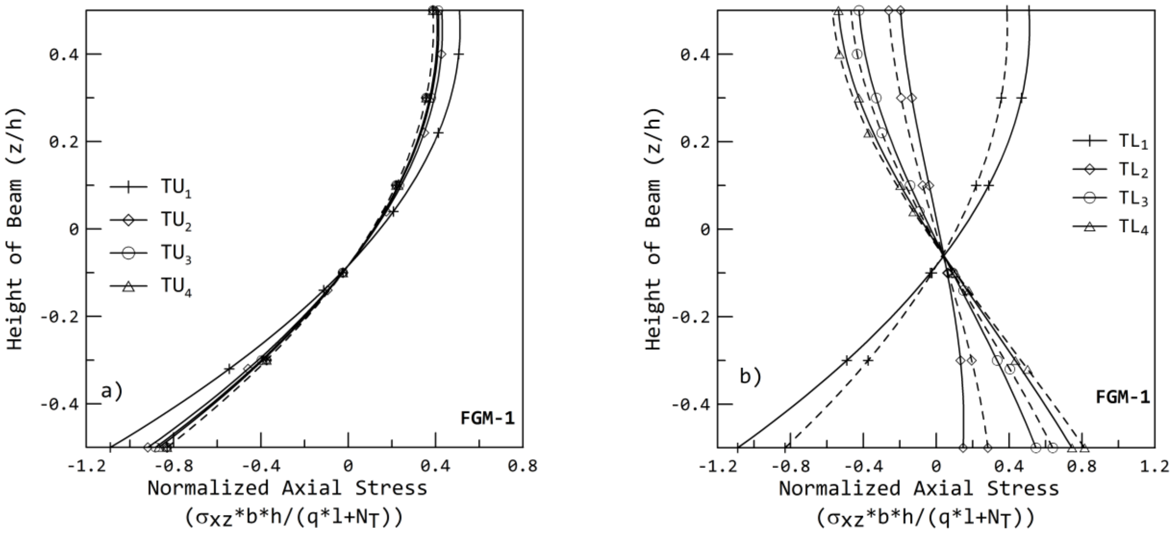

(a) (b)

Fig. 5. Axial Stresses (Normalized) at the fixed end of the C-F beam (FGM-1) for ***β***=1 a) Uniform Temperature; b) Linear Temperature Distribution

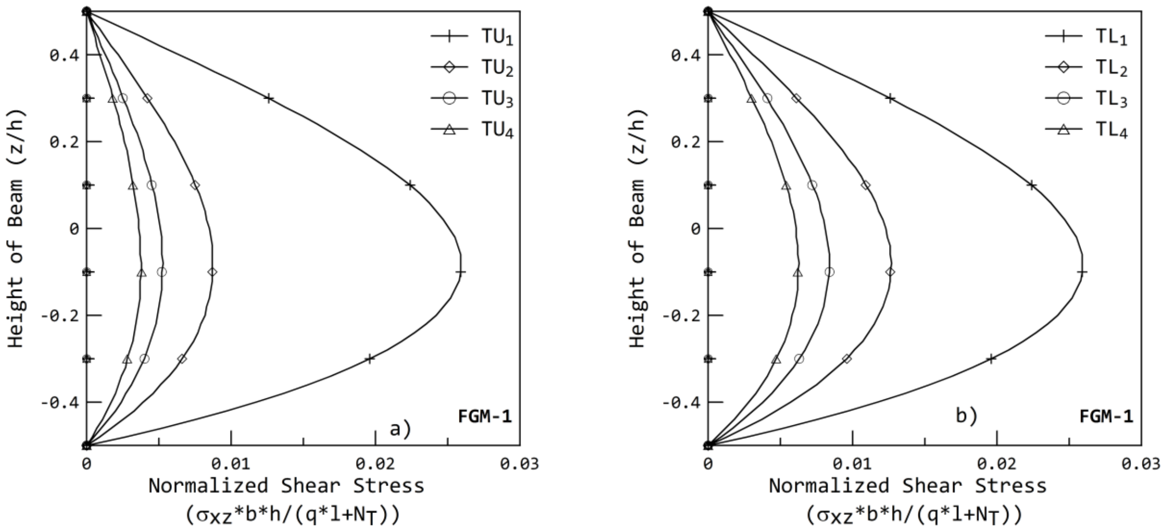

(a) (b)

Fig. 6. Shear Stresses (Normalized) at the fixed end of the C-F beam (FGM-1) for ***β***=1a) Uniform Temperature; b) Linear Temperature Distribution

Figs. 5a and 5b indicate the normalized axial stresses (maximum value at fixed end) for uniform and linear distribution, and Fig. 7c is that for nonlinear distribution. It is evident that axial stresses vary considerably with rising in temperatures.

Moreover, it is observed from Figs. 6a, 6b, and 7d that the shear stresses are same for mechanical and thermo-mechanical load. It appears as if purely thermal load does not generate any shear stress, though it is likely possible. It can be explained as the absence of thermal shear strain term while deriving the governing equations applying Virtual Work Principle. Despite that, in Fig. 6(a-b) and 7d the magnitude of shear stresses reduces with increase in temperature of bottom layer because of normalization by thermal force (N_T). It is observed from Fig. 7(b-c) that the behavior in nonlinear distribution is significantly different from uniform and linear distributions owing to the profile as presented in Fig. 7a. A significant difference in the behavior of FGM-1 under nonlinear distribution of temperature is found. In Fig. 7b the deflection of the beam is in downward direction, irrespective of the gradient.

This can be explained through the NLTD for FGM-1 depicted in Fig. 7a. It is observed that temperature variations are appreciable only for the top half of cross-section and almost constant for the bottom half. This leads to compressive stresses at the top and bottom fiber while tensile stresses in the mid-layers as presented in Fig. 7c.

In the power law expression (Eq. 1), the value of βgoverns the volume of material constituents in FGM.

As the value of*β*increase, the volume of material that forms the bottom layer increases; correspondingly the nature of FG beam follows a behavior dominated by bottom layer constituent. Table 3 reveals an idea of the percentage composition of the constituents as per the value of β. The behavior of an FG component under thermo-mechanical load with variation in volume of its constituents is significant research for its design and development. In order to gain an in depth look on the characteristics of FG beams subjected to thermo-mechanical load with different proportions of the forming constituents is reported in the following pages.

The variation of the tip deflection with the power law index for four types of temperature gradients (Table 2) with thermal and thermo-mechanical load has been plotted in Fig. 8. In Fig. 8a linear distribution of temperature (LDT) while in Fig 8b nonlinear distribution of temperature (NLDT) is contemplated. It is observed that with the increase in index value, the tip deflection first decreases up to a certain value and consequently increases for both the profiles. For LDT, as the temperature gradient increases, the tip deflection increases for the same index as well; and exhibits similar behavior for increasing index value. On the other hand, for NLDT and a specific gradient, there is a steep fall in tip deflection up to a certain index value then remains approximately constant as the index increases as depicted in Fig. 8b. In either case the thermal and thermo-mechanical plots are parallel to each other.

Table 3. Average Volume fraction of the material constituents [7]

β	V_t	V_b
0.0	1.0	0.0
0.1	0.9091	0.0909
0.5	0.6667	0.3333
1	0.5000	0.5000
1.5	0.4000	0.6000
2.0	0.3333	0.6667
3.0	0.2500	0.7500
4.0	0.2000	0.8000
15.0	0.0625	0.9375
25.0	0.0385	0.9615

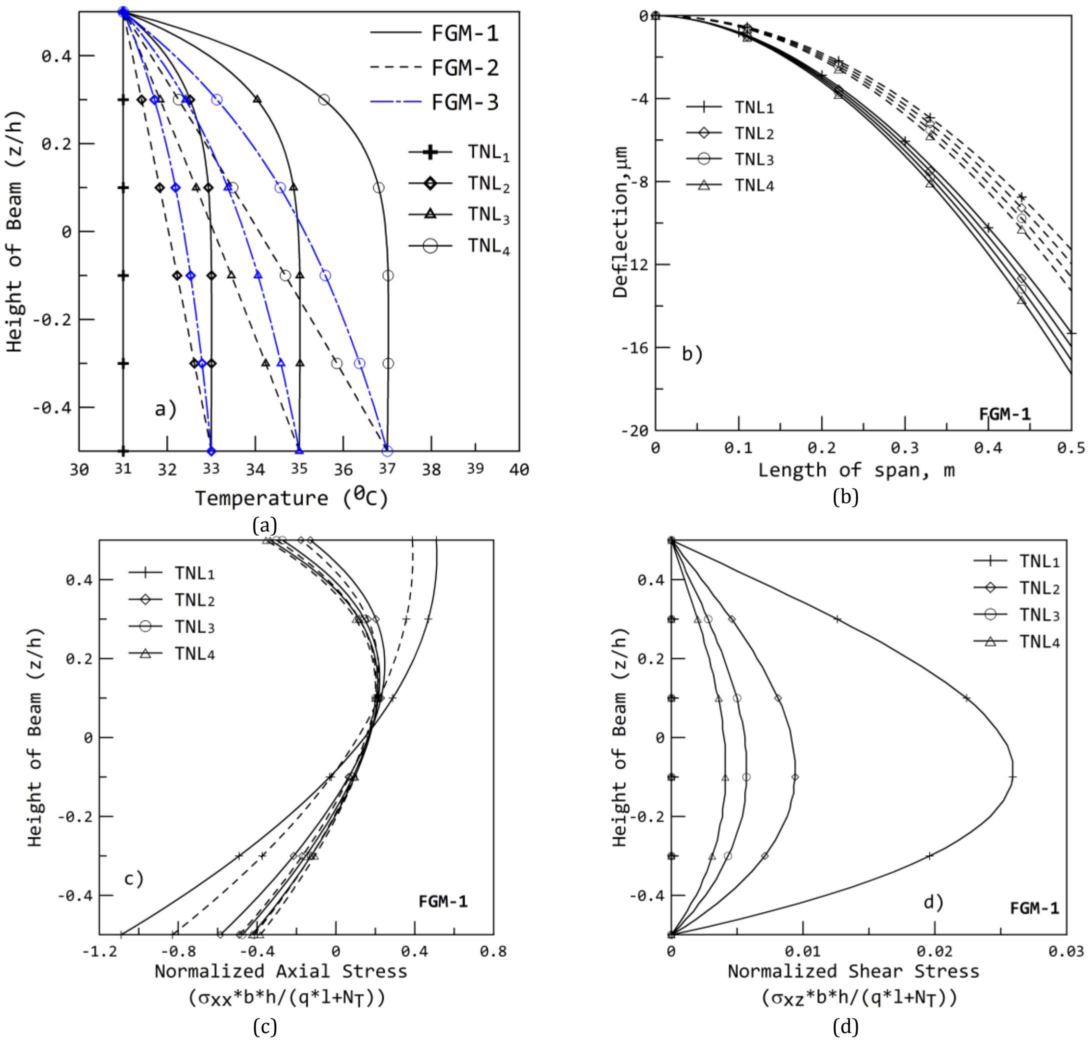

Fig. 7. For β=1& Nonlinear temperature distribution, a) Distribution of temperature across the beam height; b) Transverse Deflection; c) Normalized Axial stresses at the fixed end; d) Normalized Shear stresses at fixed end

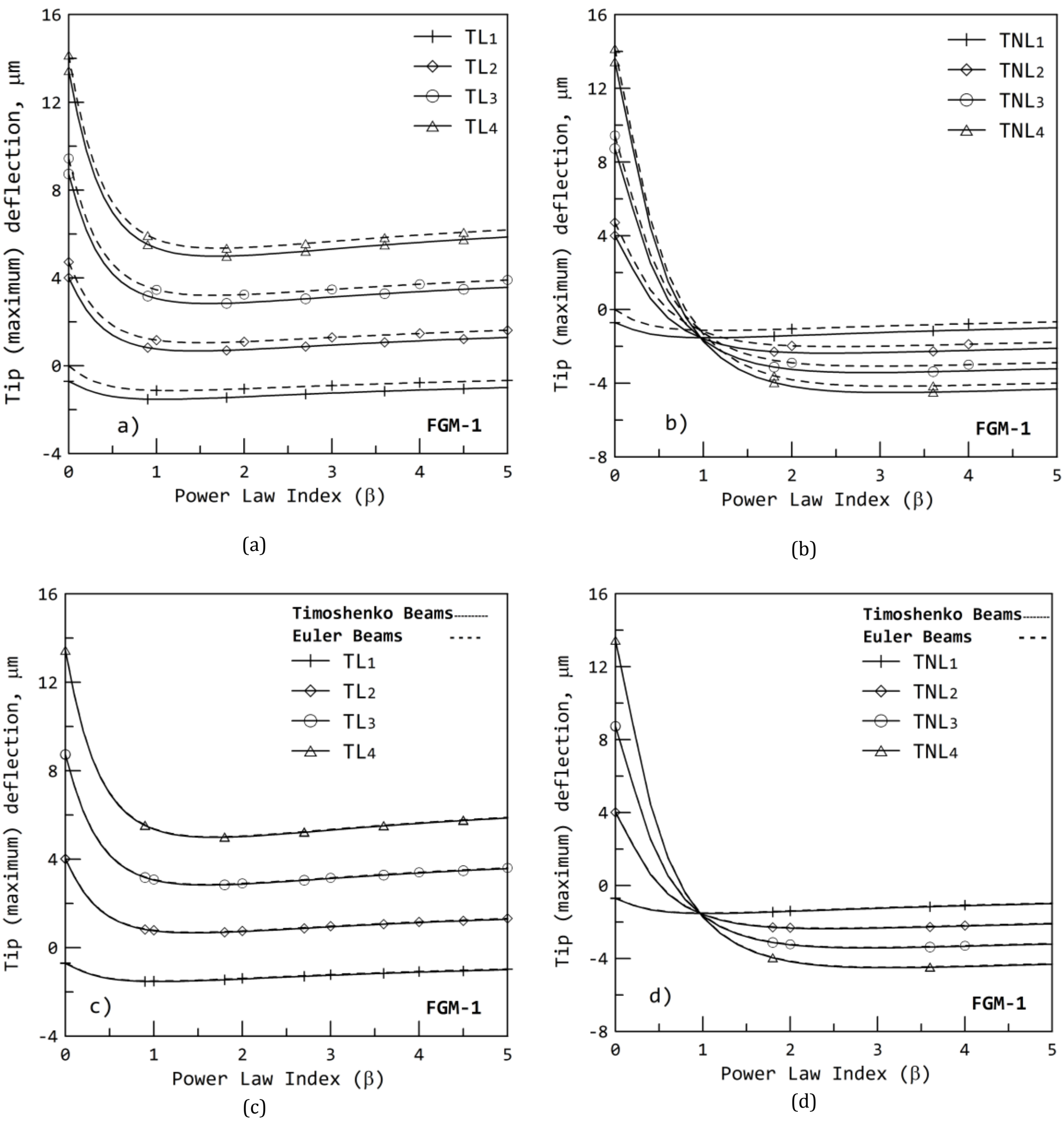

Fig. 8. Effect of shear deformation on variation in maximum (tip) deflection with (**β**)- a) LTD; b) NLTD**;** c) LTD; d) NLTD

In Fig. 8c and 8d plots to distinguish the response of Euler and Timoshenko beam under thermo-mechanical load is examined. In all the plots, the aspect (l/h) ratio is assumed to be ¼. It is observed that both the variations are very small and are insignificant which means both Euler (EBB) and Timoshenko (TB) beams respond in the same way to thermal gradient changes. The reason for such behavior is that the thermal expansion does not produce any shear deformation between the layers of beam. It is observed that the difference in deflection of EBB as well and TB is only as a result to mechanical load, and in the absence of mechanical load the response of the two is same for thermal variations. Fig. 8c shows the results for LTD while Fig. 8d for NLDT.

Fig. 9 illustrates a plot of the variation of position of neutral axis with increase in $\beta$for the three FGMs considered. The shifting in neutral axis for FGM-1 (Fig. 9) is appreciable when juxtaposed to the height of beam. The position of neutral axis is approx. 11 mm shifted below the geometrical center for a beam of height 125mm for an index value 0.85 and is roughly 9% of the beam height. On the other hand, the shifting for FGM-2 and 3 are in opposite sense, notwithstanding that the shift is relatively lesser. It is observed that the shifting of NA is a function of the modulus of elasticity of the parent materials of FGM.

The deflection and axial stress variations for a C-S and S-S beam are plotted in Figs. 10 and 11. It is observed that the deflection and stresses for C-S and S-S beams behave in similar to C-F beam as well. Despite that, they behave in opposite sense. The two ends of both C-S and S-S are constrained as a result of which the deflection initiates in the direction where the elongation is more, e.g., Aluminum with higher coefficient of thermal expansion forms the top layer. For uniform rise of temperature, the top layer elongates more; hence, the beam is deflected in upward sense. With the increase in temperature of lower layer and corresponding elongation the beam deflects downwards. The stresses plotted at the midspan reveal a corresponding behavior. The constant mechanical pressure is clearly the dissimilarity between the thermal and thermo-mechanical plots presented in Figs. 10 and 11.

The surface plots for each of the gradient case and LTD and NLTD give a rough idea of the variations of the deflections, axial stresses, and shear stresses for the FG beams (Figs. 12-14). It is observed that the variations in all types of surfaces follow a similar trend, i.e. there is a large variation up to a certain value of power law index (β=2) and for higher values of β the variations are minimal.

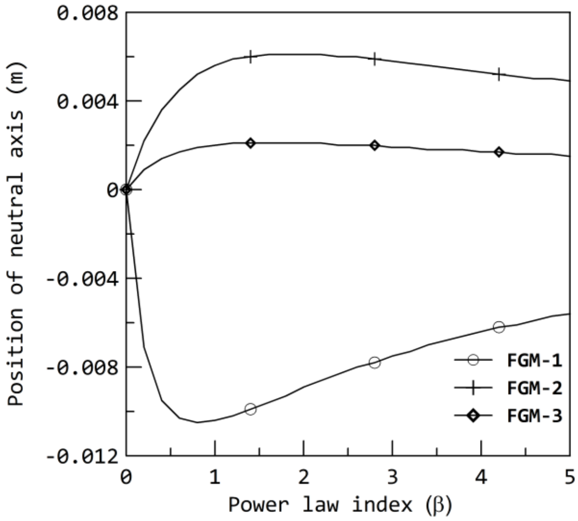

Fig. 9. Variation in the position of neutral axis with ($\boldsymbol{\beta}$)

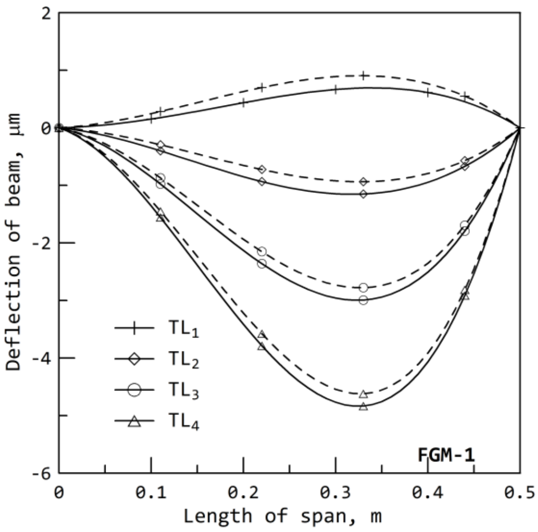

(a)

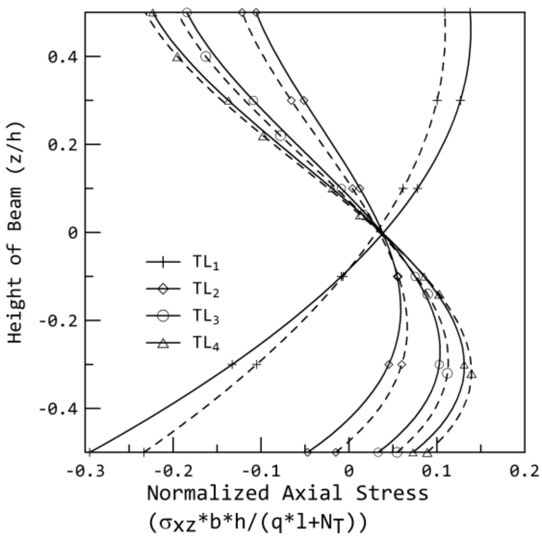

(b)

Fig. 10. C-S beam under the thermal and thermo-mechanical load of (FGM-1) for $\boldsymbol{\beta}$=1 a) Transverse Deflection; b) Normalized Axial Stress

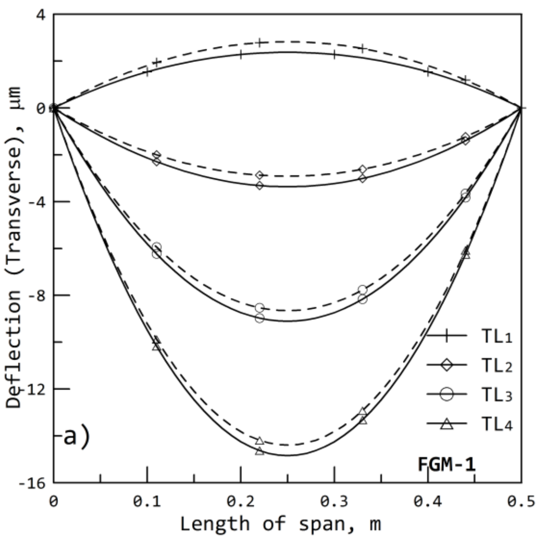

(a)

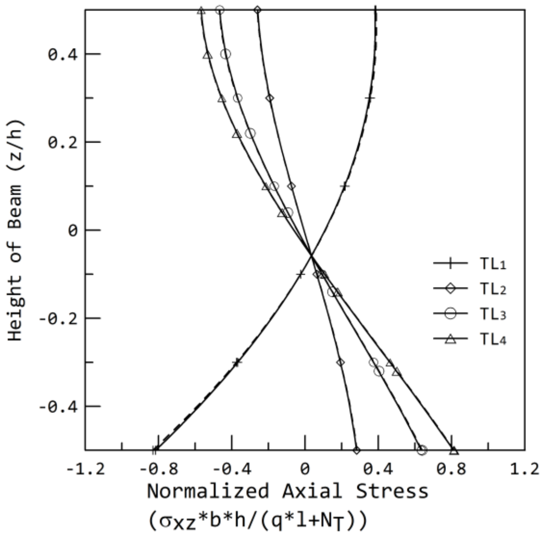

(b)

Fig. 11. S-S beam under the thermal and thermo-mechanical load of (FGM-1) for $\boldsymbol{\beta}$=1 a) Transverse Deflection; b) Normalized Axial Stress

Figures 15-17 have been plotted to compare the behavior of three different types of FG materials similarly to the change in thermal environment. Through this study, a generalized behavior of the FG beams under thermo-mechanical loading can be assessed. In the present study three combinations of five different metal/ ceramic have been simulated for deflection and stresses. In order to identify each type of combination separated denominations viz. FGM-1, FGM-2, and FGM-3 have been highlighted in the successive graphs. Both form of LTD and NLTD have been examined and investigated four types of gradients. The behavior of FGM-2 is in contrast to FGM-1, while FGM-3 behaves intermediate to both. The variation in tip (maximum) deflection, with power law index, is depicted in Fig. 15a (LTD) and 15b (NLTD). The plots may correlate to the shifting of neutral axis plotted in Fig. 9 for FGM-2 and FGM-3 as well to reveal a sharp similarity. It can be concluded that shifting of neutral axis has a major impact on the thermo-mechanical behavior of FG beams. This shifting is governed by the variation of modulus of elasticity and hence, through Eq. 1. The shifting of neutral axis is towards the side whose modulus of elasticity is higher for example for FGM-1, aluminum is on top surface and steel at bottom; hence NA shifts downwards; while for FGM-2 with silicon nitride on top which has higher value of elasticity, resulting in gaining NA upwards the geometric center line. Both LTD and NLTD display similar trends in variation with the increasing value of β. However as a result of the nonlinear profile for each FG beam (Fig. 7a) exhibits substantial difference largely due to the variation in thermal conductivity of the materials resulting in contrasting temperatures at points along the beam height. Hence it can be concluded that for nonlinear temperature variations thermal conductivity plays a vital role in accordance with elasticity modulus.

5. Conclusions

In this paper, a beam that consists of functionally graded material is deliberated to investigate its static deformation behavior under purely thermal and thermo-mechanical load. The study has its relevance in designing of an FG beam subjected to varying loading and thermal environments. How will the beam respond if the temperature on both of its surface differs from each other as well as from vicinity, with and/or without mechanical load; present research attempts to answer this question. Although a number of works, cited in the literature review, have manifested their findings relevant to thermo-mechanical loading in FG beams; the present work is unique in a way that the approach adapted in developing the governing equations formulates to a single fourth order differential equation (similar to classical beam theory for isotropic beams) acquired by substituting a dependent variable for the displacement variables.

The method was applied by Li [16] for Timoshenko beams subjected to purely mechanical load, and the present work extends the method to thermo-mechanical load, and to the best of author's knowledge, this is a novel work unpublished till date to the best of author's knowledge. The properties of material viz. elasticity modulus, rigidity modulus, coefficient of thermal expansion, and thermal conductivity are made to vary pursuant to power law function along the height of the beam assuming a constant Poisson's ratio. The beam is loaded with constant mechanical pressure on the top surface, and the temperature of top and bottom surface are assumed to be at higher value than the vicinity. The top and bottom temperatures are also kept at different values, and the temperature distribution within the beam is assumed as linear or nonlinear. The governing equations are derived applying principle of virtual work by contemplating the effect of shear deformation as well. The approach followed in the development of equations is to convert the displacement variables into a dependent variable so as in order to acquire a fourth order differential equation in terms of dependent variable. Exact solutions for different types of boundary conditions viz clamped-free simply supported, and propped cantilever has been obtained for thermo-mechanical load. A number of findings correlated to the behavior of FG beams subjected to thermo-mechanical load (linear and nonlinear temperature profiles) have been examined for varying thermal gradient and different volumes of constituents; the deflection, axial (bending) and shear stresses of such beams for a range of power law index values have been reported. Moreover, in order ro investigate the effect of different combinations of constituent materials for FGM, three combinations of materials have been examined to gain an in depth study of FG beams. The following conclusions can be enumerated in the end.

It has been observed that the deflection (transverse) of the FG beam as a result of thermal gradient starts with the slightest of the rise in surface temperature beyond the ambient value, irrespective of mechanical loading.

For the same temperature dissimilarity of the top and bottom surface, the behavior of beam is largely different for uniform, linear, and non-linear temperature profiles. The resulting behavior of beam is dependent on the directions of mechanical and thermal moment; out of these variations in thermal gradient is more critical.

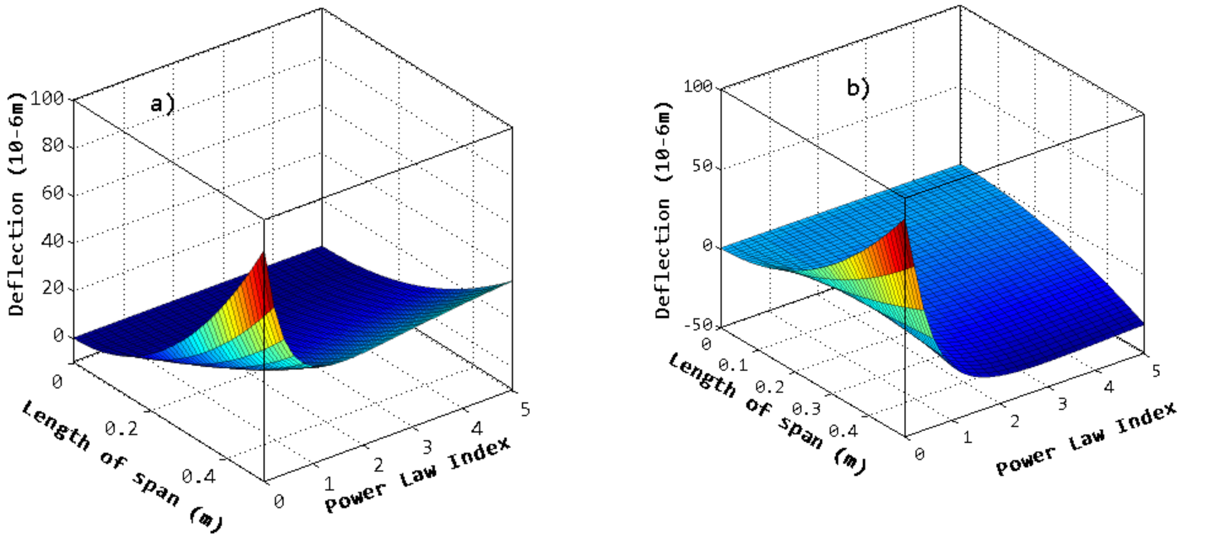

Fig. 12. Variation in transverse deflection of FGM-1 with Power law index (***β***) Linear Distribution, TL3; b)Nonlinear Distribution, TNL3

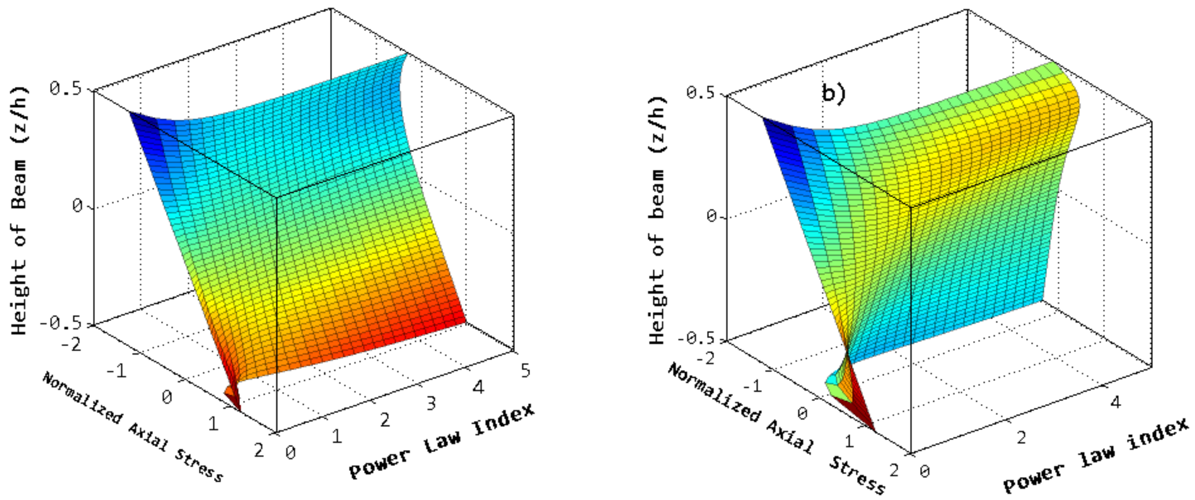

Fig. 13. Variation in normalized axial stress of FGM-1 with Power law index (***β***) a) Linear Distribution, TL3; b) Nonlinear Distribution, TNL3

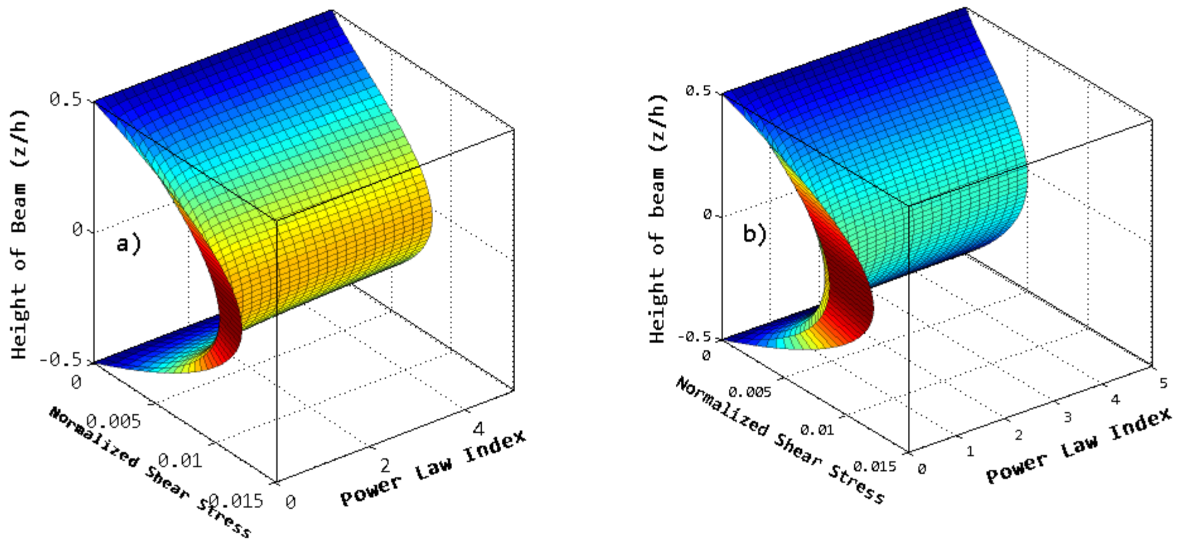

Fig. 14. Variation in normalized shear stress of FGM-1 with Power law index (***β***) a) Linear Distribution, TL3; b) Nonlinear Distribution, TNL3

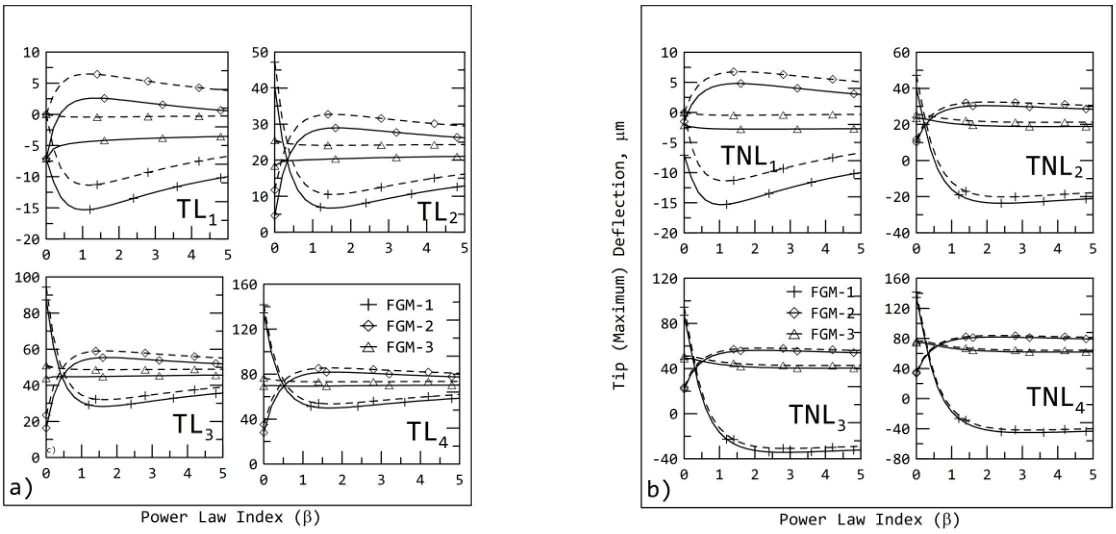

Fig. 15. Variation in transverse deflection of FGM-1 with Power law index ($\boldsymbol{\beta}$) Linear Distribution, TL3; b)Nonlinear Distribution, TNL3

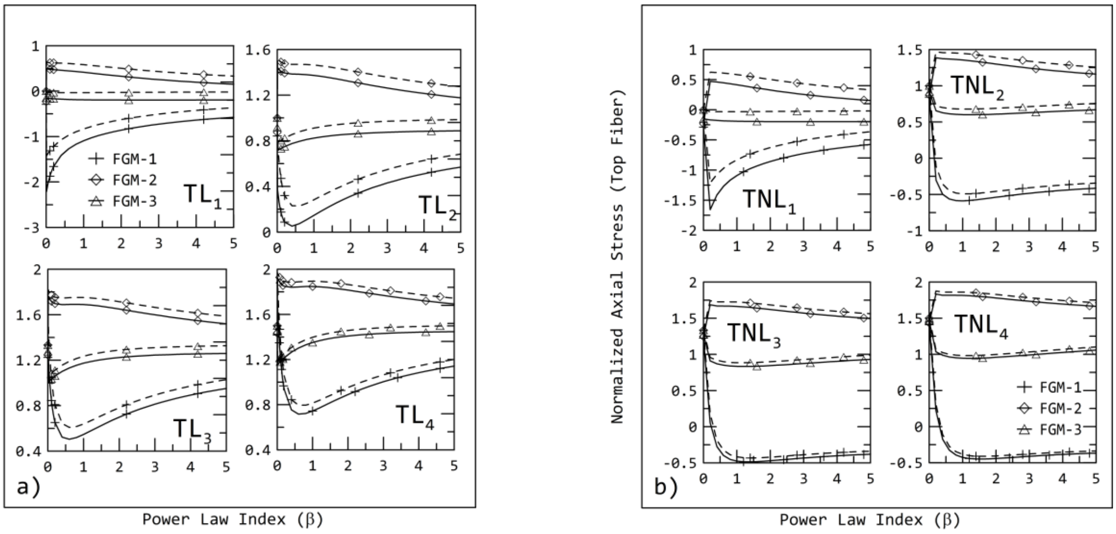

Fig. 16. Variation in normalized axial stress of FGM-1 with Power law index ($\boldsymbol{\beta}$) a) Linear Distribution, TL3; b) Nonlinear Distribution, TNL3

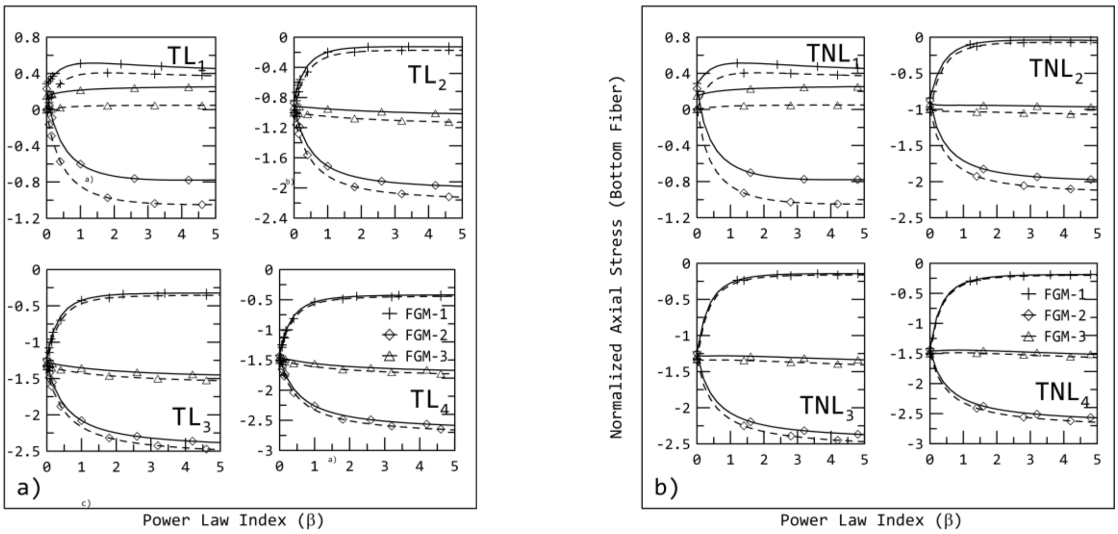

Fig. 17. Variation in normalized shear stress of FGM-1 with Power law index ($\boldsymbol{\beta}$) a) Linear Distribution, TL3; b) Nonlinear Distribution, TNL3

The thermal gradients do not produce any shear deformation (corresponding shear stresses) in the FG beam, and only mechanical load is responsible for the shear deformation. As a result, both Euler beam theory and Timoshenko beam theory for FG beam give the same result for thermal variations.

The behavior of FG beam is dependent on the loading side as well, i.e., constituent material that forms top and bottom surfaces. Both the deflection and stress profiles are dependent on the position of neutral axis which is a function of elasticity modulus of the constituents. Greater the elasticity differences the more will be the shift of neutral axis; towards the constituent with higher elasticity. The effect is observed for all types of loading conditions- mechanical, thermal and thermo-mechanical.

In case of nonlinear temperature profiles, the thermal conductivity of the parent materials plays a vital role in the behavior of FG beam. Greater the difference in thermal conductivity, the more will be nonlinearity in temperature profile. Hence if the thermal in the thermal conductivity of the constituents is less, linear profile of temperature may be assumed for simplicity even for thick beams.

Nomenclature

u, w	Linear displacement variables
ϕ	Rotational displacement variable
x, y, z	Cartesian coordinate variables
b, h, l	Width, height and length of beam
k_s	Shear correction factor
α	Coefficient of thermal expansion
β	Power law index
q	Intensity of mechanical load
T_t	Temperature of top surface,
T_b	Temperature of Bottom surface,
T_0	Surrounding temperature
E	Modulus of Elasticity
G	Modulus of Rigidity
μ	Poisson's Ratio
ϵ, γ	Axial Strain, Shear Strain
σ, τ	Axial Stress, Shear Stress
N_x	Axial Force
M_x,	Bending Moment
Q_{xz}	Shear Force
N_T, M_T	Thermal Force, Thermal Moment
TU_1,TU_2, TU_3,TU_4	Uniform Temperature Distribution
TL_1,TL_2, TL_3,TL_4	Linear Temperature Distribution
TNL_1, TNL_2, TNL_3, TNL_4	Nonlinear Temperature Distribution

References

[1] Miyamoto, Y. (Ed.), Functionally graded materials: design, processing, and applications, *Materials technology series.* Kluwer Academic Publishers, Boston; 1999.

[2] Suresh S, Mortensen A., Fundamentals of functionally graded materials. London, UK: *IOM Communications Limited;* 1998

[3] Mahamood, R.M., Akinlabi, E.T., Shukla, M., Pityana, S., Functionally Graded Material: An Overview. *Proceedings of World Congress in Engineering*; 2012; Vol.3. London UK.

[4] Udupa, G., Rao, S.S., Gangadharan, K.V., Functionally Graded Composite Materials: An Overview. *Procedia Materials Science*.; 2014; 5:1291–1299.

[5] Kieback, B., Neubrand, A., Riedel, H., Processing techniques for functionally graded materials. Materials *Science and Engineering*; 2003; A362:81–106.

[6] Birman, V., Byrd L. W., Modeling and Analysis of Functionally Graded Materials and Structures.*Applied Mechanics Reviews*; 2007; 60:195-215

[7] Reddy, J.N., Chin, C.D., Thermo-mechanical analysis of functionally graded cylinders and plates. *Journal of Thermal Stresses*; 1998; 21:593–626.

[8] Reddy, J.N., Analysis of functionally graded plates. International *Journal for Numerical Methods in Engineering*; 2000; 47:663–684

[9] Sankar, B.V., An elasticity solution for functionally graded beams. *Composites Science and Technology*; 2001; 61:89–696.

[10] Sankar, B.V., Tzeng, J.T., Thermal Stresses in Functionally Graded Beams. *AIAA Journal*; 2002; 40:1228–1232.

[11]Zhu, H., Sankar, B.V., A Combined Fourier Series–Galerkin Method for the Analysis of Functionally Graded Beams. *Journal of Applied Mechanics*; 2004; 71:421

[12] Chakraborty, A., Gopalakrishnan, S., Reddy, J.N., A new beam finite element for the analysis of functionally graded materials. *International Journal of Mechanical Sciences*; 2003; 45:519–539.

[13]Aydogdu, M., Taskin, V., Free vibration analysis of functionally graded beams with simply supported edges. *Materials & Design*; 2007;28:1651–1656.

[14] Kadoli, R., Akhtar, K., Ganesan, N., Static analysis of functionally graded beams using higher order shear deformation theory. *Applied Mathematical Modelling*; 2008; 32:2509–2525.

[15] Benatta, M.A., Mechab, I., Tounsi, A., AddaBedia, E.A., Static analysis of functionally graded short beams including warping and shear deformation effects. *Computational Materials Science*; 2008; 44:765–773.

[16] Li, X.-F., A unified approach for analyzing static and dynamic behaviors of functionally graded Timoshenko and Euler–Bernoulli beams.*Journal of Sound and Vibration;* 2008; 318:1210–1229.

[17] Kang, Y.-A., Li, X.-F., Large Deflections of a Non-linear Cantilever Functionally Graded Beam. *Journal of Reinforced Plastics and Composites*; 2010; 29:1761–1774.

[18] Birman, V., Stability of functionally graded hybrid composite plates. *Composites Engineering*; 1995; 5:913–921.

[19] Javaheri, R., Eslami, M.R., Buckling of Functionally Graded Plates under In-plane Compressive Loading.;*Math. Mech.*; 2002a 82:277-283.

[20] Praveen, G.N., Reddy, J.N., Nonlinear transient thermoelastic analysis of functionally graded ceramic-metal plates. *International Journal of Solids and Structures*; 1998; 35:4457–4476.

[21] Shen, H.-S., Nonlinear bending response of functionally graded plates subjected to transverse loads and in thermal environments. *International Journal of Mechanical Sciences*; 2002; 44:561–584.

[22] Sundararajan, N., Prakash, T., Ganapathi, M., Nonlinear free flexural vibrations of functionally graded rectangular and skew plates under thermal environments. *Finite Elements in Analysis and Design*; 2005; 42:152–168.

[23] Li, S., Zhang, J., Zhao, Y., 2006. Thermal post-buckling of Functionally Graded Material Timoshenko beams. *Applied Mathematics and Mechanics*; 2006;27:803–810.

[24] Mahi, A., AddaBedia, E.A., Tounsi, A., Mechab, I., An analytical method for temperature-dependent free vibration analysis of functionally graded beams with general boundary conditions. *Composite Structures*; 2010; 92: 1877–1887.

[25] Javaheri, R., Eslami, M.R., Thermal buckling of functionally graded plates based on higher order theory. *Journal of Thermal Stresses*; 2002b; 25: 603–625.

[26] Javaheri, R., Eslami, M.R., Thermal Buckling of Functionally Graded Plates. *AIAA Journal*; 2002c; 40: 162–169.

[27] Kiani, Y., Eslami, M.R., 2013. Thermomechanical buckling oftemperature-dependent FGM beams. *Latin American Journal of Solids and Structures*; 2013; 10:223–246.

[28]Kiani, Y., Eslami, M.R., Thermal buckling analysis of functionally graded material beams. *International Journal of Mechanics and Materials in Design*; 2010; 6:229–238.

[29] Wattanasakulpong, N., GangadharaPrusty, B., Kelly, D.W., Thermal buckling and elastic vibration of third-order shear deformable functionally graded beams. *International Journal of Mechanical Sciences*; 2011; 53:734–743.

[30] Majumdar, A., Das, D., A study on thermal buckling load of clamped functionally graded beams under linear and nonlinear thermal gradient across thickness. *Proceedings of the Institution of Mechanical Engineers, Part L: Journal of Materials: Design and Applications*; 2018; 232: 769–784.

[31] Paul, A., Das, D., Non-linear thermal post-buckling analysis of FGM Timoshenko beam under non-uniform temperature rise across thickness. *Engineering Science and Technology, an International Journal*; 2016; 19: 1608–1625.

[32] Ma, L.S., Lee, D.W., A further discussion of nonlinear mechanical behavior for FGM beams under in-plane thermal loading. *Composite Structures*; 2011; 93:831–842.

[33] Zhang, D.-G., Zhou, Y.-H., 2008. A theoretical analysis of FGM thin plates based on physical neutral surface. *Computational Materials Science*; 2008; 44: 716–720.

[34] Ma, L.S., Lee, D.W., Exact solutions for nonlinear static responses of a shear deformable FGM beam under an in-plane thermal loading. *European Journal of Mechanics - A/Solids*; 2012; 31: 13–20.

[35] Fu, Y., Wang, J., Mao, Y., Nonlinear analysis of buckling, free vibration and dynamic stability for the piezoelectric functionally graded beams in thermal environment. *Applied Mathematical Modelling*; 2012; 36:4324–4340.

[36] Fallah, A., Aghdam, M.M., Thermo-mechanical buckling and nonlinear free vibration analysis of functionally graded beams on nonlinear elastic foundation. *Composites Part B: Engineering*; 2012; 43:1523–1530.

[37] Zhang, D.-G., Zhou, H.-M., Nonlinear Bending and Thermal Post-Buckling Analysis of FGM Beams Resting on Nonlinear Elastic Foundations; *CMES, Tech Science*; 2014; 100(3):201-222

[38] Sun, Y., Li, S.-R., Batra, R.C., Thermal buckling and post-buckling of FGM Timoshenko beams on nonlinear elastic foundation. *Journal of Thermal Stresses*; 2016; 39:11–26.

[39] Niknam, H., Fallah, A., Aghdam, M.M., 2014. Nonlinear bending of functionally graded tapered beams subjected to thermal and mechanical loading. *International Journal of Non-Linear Mechanics*; 2014; 65:141–147.

[40] Nasirzadeh, R., Behjat, B., Kharazi, M., Khabazaghdam, A., Investigation of boundary condition effects on the stability of FGP beams in thermal environment. *Journal of Theoretical and Applied Mechanics*; 2017; 55(3):1003-1014.

[41] Nguyen, D.K., Bui, V.T., Dynamic Analysis of Functionally Graded Timoshenko Beams in Thermal Environment Using a Higher-Order Hierarchical Beam Element. *Mathematical Problems in Engineering*; 2017; 2017:1–12.

[42] Wallerstein, D.V., A Variational Approach to Structural Analysis. John Wiley & Sons; 2002

[43] Dym, C.L., Shames, I.H., Solid mechanics: a variational approach, Augmented edition. ed. *Springer Science+Business Media, New York.*2013